Journal of Cleaner Production 294 (2021) 126300

Contents lists available at ScienceDirect

Journal of Cleaner Production

journal homepage: www.elsevier.com/locate/jclepro

# Toward recycling "unsortable" post-consumer WEEE stream: Characterization and impact of electron beam irradiation on mechanical properties

Imane Belyamani [a, *], Joachim Maris [b, c], Sylvie Bourdon [b], Jean-Michel Brossard [b], Laurent Cauret [a], Laurent Fontaine [c], Véronique Montembault [c, **]

[a] Institut Supérieur de Plasturgie D'Alençon (ISPA), Pôle Universitaire de Montfoulon, BP 823, 61041; Alençon Cedex; France
[b] Veolia Recherche et Innovation, Zone Portuaire de Limay, 291 Avenue Dreyfous-Ducas, 78520; Limay; France
[c] Institut des Molécules et Matériaux Du Mans (IMMM) - UMR 6283 CNRS, Le Mans Université, Avenue Olivier Messiaen, 72085 Le Mans Cedex 9; France

ARTICLE INFO

*Article history:*
Received 31 July 2020
Received in revised form
28 January 2021
Accepted 5 February 2021
Available online 8 February 2021

Handling editor: Dr Sandra Caeiro

*Keywords:*
Unsortable plastics
Post-consumer WEEE
Electron beam irradiation
Sampling method
Plastics recycling
Mechanical properties

ABSTRACT

The work reported here is the first study aimed at providing a full screening of a real unsortable non-recycled post-consumer WEEE stream free of brominated flame retarded plastics, separated using on-line X-ray detection, toward its recycling. In the existing sorting lines, up to 40% of plastics from waste electrical and electronic equipment (WEEE) stream can be rejected, herein named unsortable plastics. To have the most representative homogeneous sample for physico-chemical characterizations, a sampling method was developed to overcome the heterogeneity of the investigated 500 kg batch. The batch screening on both representative samples (~500 μm size) and 100 plastic fractions (~20 mm size), by means of routine techniques used in the plastic industry, has allowed to quantify reliably the main polymers included in the studied batch; ~50% styrene-based polymers, ~15% polypropylene (PP), ~15% polycarbonate (PC), ~1–4% polyamide (PA), polyethylene (PE), polyvinyl chloride (PVC), poly (ethylene terephthalate) (PET), poly (methyl methacrylate) (PMMA) and ~8% of multi-layer plastics, paints and thermosets. The identification of the ~8.0% inorganic phase by X-ray fluorescence spectrometry revealed the presence of several additives/charges commonly incorporated in plastic materials, such as calcium carbonate and talc. The studied batch was then subjected to electron beam irradiation at 50 and 200 kGy doses, as a means of compatibilization between the batch components. The mechanical properties and thermal behavior of irradiated samples pointed out the crucial role of the residual free radical scavenger agents present in post-consumer WEEE streams, leading to significantly different properties compared to those of irradiated virgin polymer blends highlighted in the literature.



## 1. Introduction

Waste electrical and electronic equipment (WEEE) is the fastest growing source of waste, potentially rising 4% per year (Sahajwalla and Gaikwad, 2018). This increasing waste stream has led to the publication of directive 2012/19/EU by the European Commission, targeting a WEEE recycling rate between 55% and 80% (2012/19/EU, 2012). WEEE is a complex stream consisting of a mixture of metals (Kyere et al., 2018), ceramics, glass and plastics. The proportion of the latter, depending on the six WEEE categories defined in directive 2012/19/EC (2012/19/EU, 2012), is ranging between 10 wt% and 33 wt% (Gramatyka et al., 2007; Kang and Schoenung, 2005; Parajuly and Wenzel, 2017; Vazquez and Barbosa, 2016; Wang and Xu, 2014; Widmer et al., 2005). Therefore, to achieve the objectives set out in directive 2012/19/EC, WEEE plastic recycling is imperative. Furthermore, plastic waste management has become an ecological issue given the need to limit the impact of plastics on our environment (Dolores et al., 2020; Hamaide et al., 2014; Ismail and Hanafiah, 2019; Milad et al., 2020). From an economical point of view, studies on the plastic composition in WEEE reported in the literature highlighted the presence of different types of polymers, the amount of which varies with the source (Alwaeli, 2011; Bovea et al., 2016; Chancerel and Rotter, 2009; Dimitrakakis et al., 2009;

* Corresponding author.
** Corresponding author.
*E-mail addresses:* imane.belyamani@zu.ac.ae (I. Belyamani), veronique.montembault@univ-lemans.fr (V. Montembault).

https://doi.org/10.1016/j.jclepro.2021.126300

Maris et al., 2015; Martinho et al., 2012; Stenvall et al., 2013; Taurino et al., 2010). Considering the economic effectiveness of the waste utilized as substitutes for primary materials, as discussed by Alwaeli (2011), only the most representative polymers of the stream, that can be technically sorted and valorized according to the regulatory, are separated individually for further mechanical recycling operations. The plastic composition of WEEE issued from small electrical and electronic equipment (EEE) recycling units in Europe consists mainly of acrylonitrile-butadiene-styrene copolymer (ABS), polypropylene (PP), polystyrene (PS), and high-impact polystyrene (HIPS) (Dimitrakakis et al., 2009; Maris et al., 2015; Martinho et al., 2012). Up to now, the complexity and financial cost of plastic sorting makes difficult to consider the separation of the plastics from each other to facilitate recycling of a single type of polymer.

In the past decade, near infrared spectroscopy (NIR) has been integrated in the recycling process of WEEE (Menad, 2016), and allows to separate automatically on line the ABS, PP and PS from waste white plastics with a high accuracy up to 99% (Li et al., 2019). This technique can potentially detect other plastics. However, it is not always relevant to the amount of each plastic and the economic issues related to sorting schemes. As a result, about 40% of WEEE plastics are rejected from the sorting line, herein named unsortable (Fig. 1), because i) they do not comply with sorted resins, ii) they contain dark pigments, named black plastics (Maris et al., 2015), which are not recognized by the classical NIR equipment or iii) because they contain brominated flame retardants (BFR), estimated to be ~25% of WEEE plastics (Hennebert, 2017). Using on-line X-ray detection, BFR-containing plastics are separated as specified in the directive 2019/1021/EU (2019/1021/EU, 2019). Indeed, the recovery of brominated flame retarded plastics has been restricted to treatments that destroy or irreversibly transform the substances, as stated in 2012/19/EC directive and Stockholm convention (2012/19/EU, 2012; Stockholm Convention, 2017).

Based on this observation, Tostar et al. (2016) have studied recycling of a polymer blend based on 80 wt% styrene-based polymers and 10 wt% PP from WEEE, by adding a compatibilizer or by gamma irradiation. The irradiation of polymeric materials with ionizing radiation appears to be a promising tool to chemically modify polymers as it leads to the formation of free radicals along the backbone even on low reactive polymers, such as polyolefins (Burillo et al., 2002; Chmielewski et al., 2005). The compatibilization is ensured by i) direct crosslinking between macroradicals of two polymers to form new covalent bonds (Gu et al., 2014; Li et al., 2009) or ii) indirect crosslinking via a coupling agent binding two polymers (Lambla and Seadan, 1992, 1993; Xanthos and Dagli, 1991). The resulting copolymers act as a compatibilizing agent which concurrently lower the interfacial tension at phase boundaries and enhance their adhesion, leading to an improvement of the mechanical properties (Maris et al., 2018; Utracki, 2002). For example, the mechanical properties of a blend of seven virgin polymers frequently found in plastic solid waste: low-density polyethylene (LDPE), high-density polyethylene (HDPE), poly (vinyl chloride) (PVC), PS, HIPS, PP, and poly (ethylene terephthalate) (PET) were improved through the addition of peroxides (Vivier and Xanthos, 1994). Similarly, Said et al. (2013) have reported an enhancement of the tensile properties of different PET/LDPE mixture compositions subjected to gamma irradiation at 25 and 50 kGy doses. Blends of waste polyethylene/LDPE 70/30, exposed to electron beam (EB) irradiation at doses up to 300 kGy, showed higher ductility, toughness, and resistance to oxidative degradation. These irradiated blend materials were successfully blow molded to make bottles (Satapathy et al., 2006).

Apart from Taurino et al. (2010) investigations on characterization of two sorted black/grey plastic waste categories (i.e. personal computers and televisions), the work reported in this article is the first study aimed to analyze and provide a full screening of a real unsortable non-recycled post-consumer WEEE stream.

In this contribution, for the first time the composition of unsortable post-consumer WEEE plastics stream free of BFR, sorted using on-line X-ray technique as specified in the directive 2019/1021/EU, was investigated. The studied 500 Kg batch was collected in France from the following streams: cooling appliances, household electrical equipment, and information technology (IT), such as computers, printers and phones. The polymer and additives/charges composition of unsortable plastics has been determined using Fourier-transform infrared (FTIR) spectroscopy, X-ray fluorescence spectrometry, differential scanning calorimetry (DSC), and thermogravimetric analysis (TGA).

Burillo et al. (2002); Fel et al. (2016); Lambla and Seadan (1993); Numata and Fujii (1995); Said et al. (2013); Satapathy et al. (2006); Tostar et al. (2016); Vivier and Xanthos (1994) have reported the impact of irradiation process on polymer blend. In contrast to these cited studies where polymer blend recycling was simulated on the

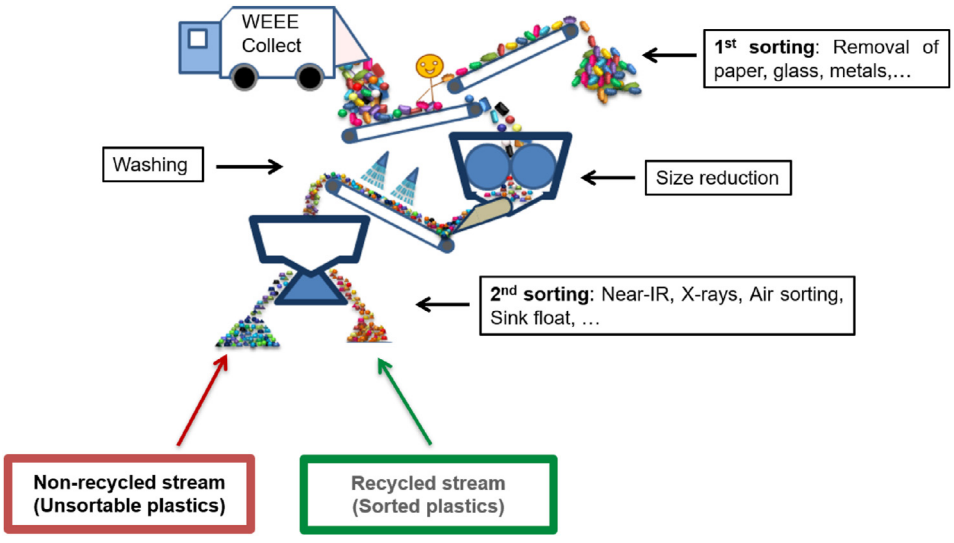


**Fig. 1.** General sorting steps for post-consumer WEEE plastic waste.

basis of virgin polymers or unsorted plastics, the present work provides a comprehensive investigation on EB-irradiated unsortable post-consumer WEEE batch prior to melt-process. EB irradiation has the advantage of being a clean and continuous process that is already commercially well-established (Drobny, 2010). Thus, the impact of EB irradiation doses (50 and 200 kGy) on thermal behavior and mechanical properties of the studied batch was investigated.

## 2. Experimental section

### 2.1. Materials

A 500 kg big bag of unsortable post-consumer WEEE, collected in April 2015, was supplied by Veolia (France). Liquid nitrogen used to grind the sample was provided by Air Liquide (France).

### 2.2. Sampling procedure

The sampling procedure was carried out on a 500 kg batch with heterogenous fraction sizes (<70 mm) from unsortable post-consumer WEEE stream. In order to have the most representative homogeneous sample for physico-chemical characterizations, a sampling method is necessary to overcome the heterogeneous constitution and size distribution of the tested batch. For this study, we developed a sampling method (see Fig. 2) based on Gy (1998) work and the XP CEN/TS 17188 standard (Afnor, 2018), and adapted from our research team previous work (Epsztein et al., 2014).

### 2.3. Melt processing and characterization methods

#### 2.3.1. Twin-screw extrusion

Extrusion experiments were carried out using a co-rotating twin-screw extruder Coperion ZSK18 (L/D = 40). The barrel temperature along the interpenetrate screws (feeding to die) was set at 190, 190, 200, 200, 200, 200, 200, 210, 210 and 210 °C with a screw speed of 250 rpm. The obtained extrudates were pelletized after cooling.

#### 2.3.2. Injection molding

Dog-bone specimens 1A ISO 527 type and impact bars (80 x 10 × 4 $mm^3$) were injection molded using a Krauss Maffei EX80-380 injection molding extruder. The detailed processing parameters are summarized in Table S1.

#### 2.3.3. Fourier-transform infrared spectroscopy (FTIR)

Infrared spectra were collected in the wavenumber range 400−4000 $cm^{-1}$ using a Fourier transform spectrometer Nicolet 380 DTGS in transmission mode for micro-ground samples, and ATR (attenuated total reflection) mode for bulk samples. Spectra were recorded at a resolution of 2 $cm^{-1}$ and 128 scans. The pellet samples for the transmission mode were prepared by grinding micro-ground sample (~500 μm) and KBr powder with a ratio of 10:100, and then pressing the mixture into pellets.

#### 2.3.4. Differential scanning calorimetry (DSC)

Differential scanning calorimeter analysis was carried out on ~7 mg representative sample using a Q100 TA Instrument under standardized conditions ISO 11357. Samples were equilibrated at −50 °C, ramped at a heating rate of 10 °C/min to 280 °C, cooled down to −50 °C and re-heated to 280 °C at the same heating rate, under nitrogen atmosphere. The reported data represent the cooling and the second heating cycles for three replicates.

#### 2.3.5. Thermogravimetric analysis (TGA)

Thermal behavior of the studied samples was investigated on ~13 mg representative sample, following the ISO 11358 standard, using a TGA1 analyzer from Mettler Toledo. Tests were performed from 50 to 900 °C under nitrogen atmosphere (flow of 45 mL/min) at a heating rate of 10 °C/min. After 1 min isothermal at 900 °C under nitrogen, the atmosphere was switched to dry air and kept for 10 min at 900 °C. The repeatability of the measurement was evaluated on the basis of three replicates.

#### 2.3.6. Energy dispersive X-ray fluorescence (XRF)

The XRF data were collected with a wavelength dispersive X-ray spectrometer PW2404-DY 750 Philips equipped with a rhodium X-ray tube anode and operated at 2.4 kW power for all measurements using vacuum conditions. To investigate possible interferences, different scans were performed using a 27 mm collimator and five crystals: LiF 200, LiF 220, Ge, InSb and PX1. The XRF test specimens were obtained by compression molding the representative sample powder at 160 °C, under manual pressure of ~15 bars. The reported values represent the average of three replicates.

#### 2.3.7. Electron beam irradiation

EB irradiation was performed on extruded pellets and micro-ground samples by Ionisos SA (France) using a commercial EB accelerator source of $^{60}Co$, under room temperature and air atmosphere. The tested irradiation doses (50 and 200 kGy) were controlled by varying the automatic conveyor speeds. Acceleration energy was set at 0.7 ± 0.2 MeV.

#### 2.3.8. Tensile strength

Tensile strength tests were carried out on injection molded dog-bone specimens 1A ISO 527 type, according to ISO 527 standard, using MTS Criterion® 43 test machine. Samples were equilibrated at ~23 °C and ~50% relative humidity (RH) for at least 48h before testing them under the same environmental conditions. The reported values represent the average of ten replicates for tensile stress and tensile stains, and of five replicates for Young moduli.

#### 2.3.9. Impact toughness

Horizontal Charpy impact tests were carried out as per ISO 179 standard on unnotched injection molded sample bars, using ZWICK 5102.202 impact pendulum device. Samples were equilibrated at ~23 °C and ~50% RH for at least 48h before testing them under the same environmental conditions. The reported impact toughness values were calculated for ten replicates.

## 3. Results and discussion

### 3.1. Composition of the studied unsortable WEEE batch

Being aware of the composition and fraction size distribution (<70 mm) heterogeneity of the studied batch, a sampling method turned out to be necessary to obtain the most representative sample from the supplied big bag. Thus, we adapted a sampling method based on our research team previous work (Epsztein et al., 2014), as detailed in Fig. 2.

The 500 kg batch was first spread out and divided into four quarters twice, and at each time, only two quarters were retained to finally obtain a 125 kg batch sample. After a manual sorting, aimed at removing residual metals, glass, paper … etc, the sample batch was ground to a particle size of ~20 mm, and three ~50 g samples were collected from the pallet box central horizontal axis using a sampling probe. The three collected samples were mixed, ground to a particle size of 2−4 mm, then to 500 μm. Finally, the ~150 g sample was divided using a rotating divider to obtain

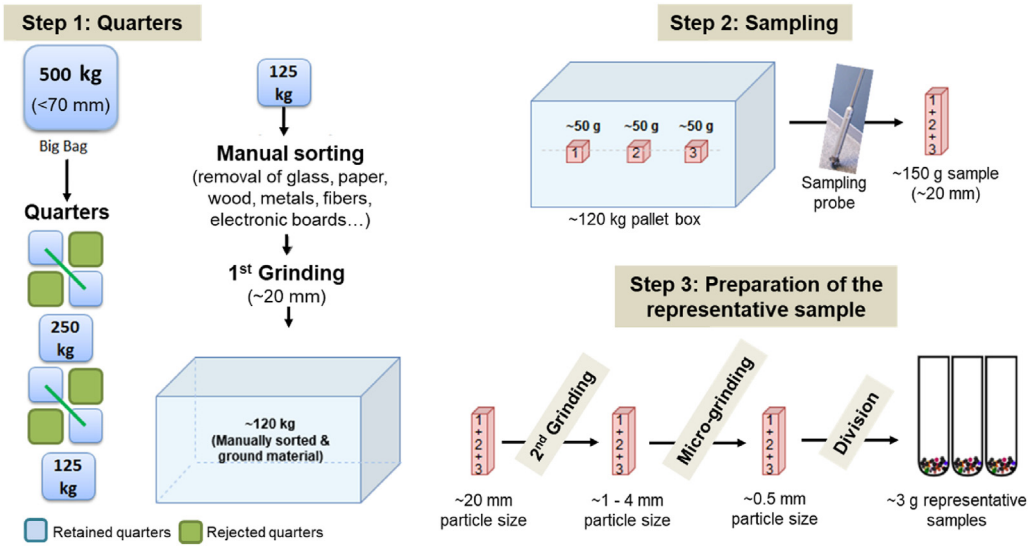


**Fig. 2.** Sampling method used in the present study.

homogeneous representative sample fractions, of approximately 3 g, used for physico-chemical analysis.

### 3.1.1. Analysis of bulk samples

In order to quickly estimate the composition of the studied unsortable batch, 100 ground samples of ~20 mm size (Fig. 3a) were collected arbitrary from the ~120 kg pallet box (Fig. 2) and characterized by attenuated total reflection Fourier-transform infrared spectroscopy (ATR-FTIR). The polymer nature corresponding to each plastic fraction was identified by comparing the recorded ATR-FTIR spectra to that of the Omnic software database. Fig. 3b depicts the sum of assigned spectral polymers gathered from the 100 analyzed samples.

The composition heterogeneity of the batch under investigation is clearly seen in Fig. 3. The collected sample is mainly constituted of styrene-based polymers (~50%) such as acrylonitrile-butadiene-styrene (ABS), polystyrene (PS), high impact polystyrene (HIPS), poly (styrene-*co*-acrylonitrile) (SAN) and poly (styrene-*co*-butadiene) (SB). Polypropylene (PP) and polycarbonate (PC) represent about 15% each. Polyamide (PA), polyethylene (PE), polyvinyl chloride (PVC), poly (ethylene terephthalate) (PET) and poly (methyl methacrylate) (PMMA) are present in a very low quantity (i.e. 1-4%). It is worth noting that the ~8% of "other polymers" include unidentified polymers such as multi-layer plastics, paints and thermosets. This preliminary polymer identification (Fig. 3) allows to determine qualitatively the polymer composition in the batch. Although this identification cannot be considered as representative of the batch, the obtained results agree well with the data reported by Maris et al. (2015). Similarly, other studies carried out in Germany (Dimitrakakis et al., 2009), and Portugal (Martinho et al., 2012) on post-consumer plastic waste batches derived from small EEE showed that ABS, PS/HIPS (~50–56 wt%) and PP (~25–30 wt%) account for at least 70 wt% of the total plastic weight, and that the weight percent of each polymer depends on the equipment type and WEEE categories (e.g. small household appliances, IT devices …).

### 3.1.2. Analysis of the batch representative sample

Likewise, the representative sample was characterized using FTIR, in the transmission mode, differential scanning calorimetry (DSC), thermogravimetric analysis (TGA) and energy dispersive X-ray fluorescence (XRF) to identify more reliably and quantitatively the composition of the studied batch before its melt processing and for further mechanical characterization. Through the different cited physico-chemical analysis, the following polymers, additives, charges and fillers were identified.

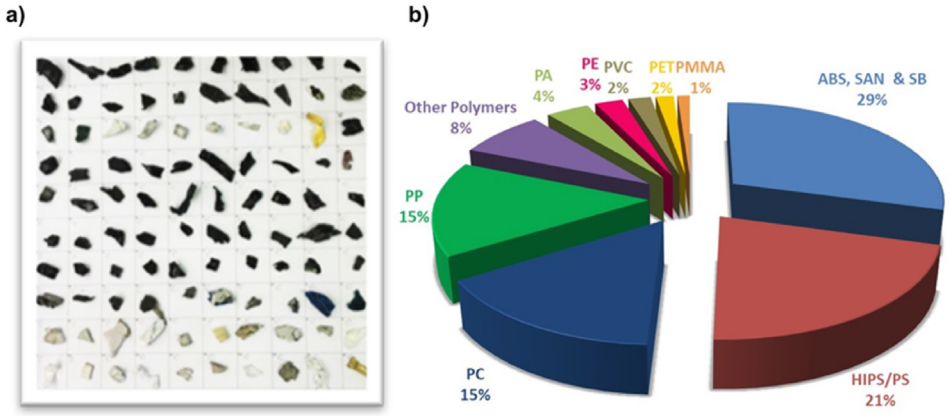


**Fig. 3.** a) 100 ground samples of ~20 mm size used to estimate b) the polymer composition, in %, of the studied unsortable batch using ATR-FTIR analysis.

*3.1.2.1. Styrene-based polymers.* Table 1 presents the absorption bands observed on the FTIR transmission spectral signature (Fig. S1) and their assignment for the studied batch representative sample. It is clearly seen that the main screened constituents are styrene-based polymers. Indeed, the strong out-of-plane C–H bending bands at 697 and 757 $cm^{-1}$, and the aromatic C–C stretching bands at 1452, 1493 and 1601 $cm^{-1}$ are characteristic of the aromatic substitution pattern. Additionally, the two (out of four) aromatic combination bands in mono-substituted benzene (1879 and 1941 $cm^{-1}$), usually observed for PS (Liang and Krimm, 1958; Munteanu and Vasile, 2005), confirm the presence of styrene pattern. The other two aromatic combination bands (1745 et 1800 $cm^{-1}$) might be hidden due to the band overlapping as a consequence of the complex composition of the studied batch.

On the other hand, the absorption peaks of butadiene pattern recorded at 967 and 909 $cm^{-1}$ are representative of ABS, SB and/or HIPS; these polymers are mainly characterized by C–H deformation in *trans*-1,4-butadiene isomer and in 1,2-butadiene units at 965 and 910 $cm^{-1}$ respectively. The other butadiene characteristic band (i.e. 729 $cm^{-1}$ for δ $CH_2$ in *cis*-1,4-butadiene) (Lacoste et al., 1996; Silas et al., 1959) could not be detected. Nevertheless, the peak at 1640 $cm^{-1}$ reflects the stretching vibrations of the C=C interaction in the 1,2-butadiene group (Munteanu and Vasile, 2005). Adding to that, the stretching vibrations of the nitrile group (C≡N), typical for ABS and SAN, was observed at 2236 $cm^{-1}$.

The presence of styrene-based polymers in the studied batch is also supported by DSC (Fig. 4a). As it is clearly seen in Fig. 4a, a glass transition temperature ($T_g$) around 99 °C, distinctive of ABS, PS, HIPS and SAN, was identified.

*3.1.2.2. Polyolefins.* The DSC thermograms (Fig. 4a) depict two distinctive endothermic peaks at ~129–133 °C and ~162–165 °C, typical of PE and PP melting temperatures ($T_m$ *PE* and $T_m$ *PP*), respectively. Besides, the cooling exotherms in Fig. S2 display two single crystallization peaks at temperatures corresponding to PP (*Tc* = ~120–121 °C) and PE (*Tc* = ~144–146 °C). Moreover, compared to the PP crystals melting enthalpy (~5.9–8.3 J/g), that of PE (~0.3–2.7 J/g) indicates a very low weight concentration of PE in the studied batch, which perfectly matches the FTIR data for bulk samples (Fig. 3b).

Interestingly, a higher temperature melting peak next to the main PP endothermic peak was observed at ~175 °C for two replicates (Fig. 4a). It is not clear whether this extra melting peak is a consequence of different PP lamellar arrangements that may result from polymer oxidation phenomenon, or simply the presence of α-phase isotactic PP crystals (Huy et al., 2004) subsequent to different crystallization conditions that may have occurred during the manufacture processes.

*3.1.2.3. Other polymers*

***Polyamides.*** The maximum absorption peak at ~3298 $cm^{-1}$ (Table 1 and Fig. S1) could be assigned to stretching vibrations of NH bond, characteristic of polyamides. However, it has been shown that the degradation of ABS can lead to the OH moiety formation with a vibration band at ~3400 $cm^{-1}$ (Li et al., 2017). Furthermore, the large melting peak at ~220 °C (Fig. 4a) and the crystallization one at ~190 °C (Fig. S2) can be attributed to PA6, PA610 and/or PA612.

***PC, PMMA, PET.*** The very low concentration of PMMA and PET in the studied batch (Fig. 3b) as well as the hiddenness of the PC $T_g$, covering the 145–150 °C range, by other polymers thermal events (Fig. 4a and Fig. S2) make their detection by DSC impossible. Nonetheless, Fig,. S1 and Table 1 exhibit several absorption peaks that may be associated with PC, PMMA or PET. Bands at 1772 $cm^{-1}$, assigned to stretching vibrations of C=O bond, and the absorption peaks between 1128 and 1235 $cm^{-1}$ (Fig. S1), corresponding to stretching vibrations of C–O bond, involve the presence of PC (Ghorbel et al., 2014). The band at 1731 $cm^{-1}$ can also be attributed to stretching vibrations of C=O interactions of the ester function in PET or PMMA (Ghorbel et al., 2014; Zhu and Kelley, 2005).

Although the mentioned absorption peaks emphasize the presence of PC, PMMA and PET, the same functional groups can also be ascribed to the degradation of styrenic polymers, either via thermo- (Karahaliou and Tarantili, 2009; Vilaplana et al., 2006) or photo-oxidation (Gardette et al., 1995) mechanisms.

**Table 1**
Observed FTIR absorption bands and their assignment for the representative sample of the studied unsortable WEEE batch.

| Wavenumber ($cm^{-1}$) | Intensity | Assignments | Polymer type |
|---|---|---|---|
| 697 | vs | δ C-H aromatic | Styrene-based polymers |
| 757 | m | | |
| 1452 | m | ν C-C aromatic | Styrene-based polymers |
| 1493 | w | | |
| 1601 | w | | |
| 1879 | vw | Aromatic combination bands in mono-substituted rings | PS |
| 1941 | vw | | |
| 2236 | vw | ν C≡N | ABS, SAN |
| 3025 | w | ν C-H aromatic | Styrene-based polymers |
| 3059 | vw | | |
| 1640 | w | ν C=C of 1,2-vinyl butadiene | ABS, HIPS, SB |
| 909 | w | δ $CH_2$ 1,2-butadiene | |
| 964 | w | δ $CH_2$ *trans*-1,4-butadiene isomer | |
| 1163 | m | ν C-O & ν C-C aromatic | PC |
| 1193 | m | | |
| 1229 | m | ν C-O | |
| 1772 | w | ν C=O | |
| 1731 | w | ν C=O | PET or PMMA |
| 1376 | w | δ $CH_3$ | PP |
| 2849 | w | ν $CH_2$ polymer chains | PE |
| 2917 | m | | |
| 3298 | vw | ν NH or ν OH | PA or degraded ABS respectively |

vs: very strong; m: medium; w: weak; vw: very weak; ν: stretching vibrations; δ: bending vibrations

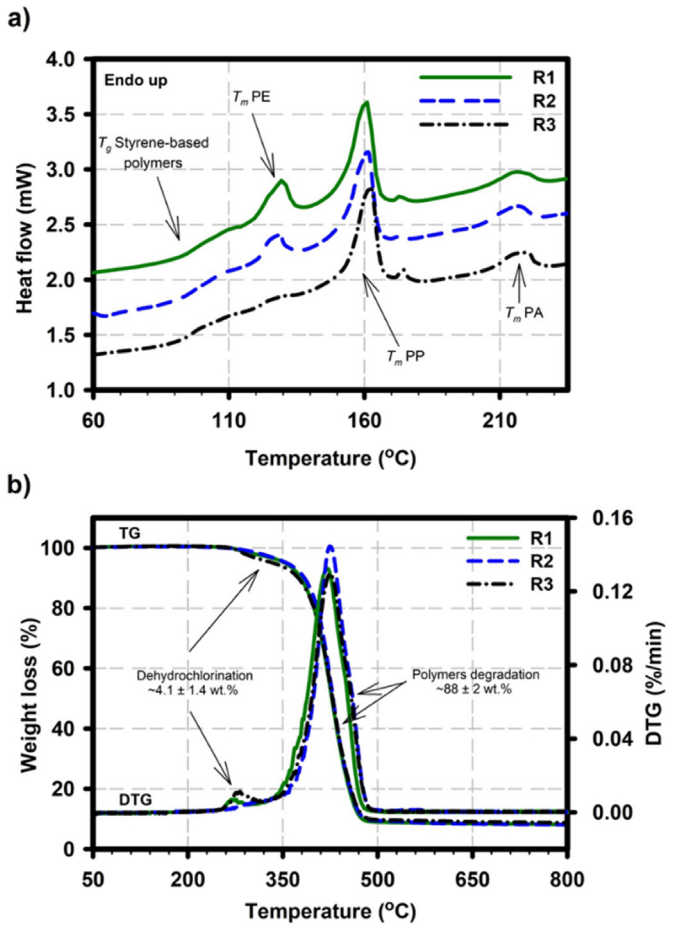


**Fig. 4.** a) 2nd heating DSC thermograms, and b) TG and DTG curves for three replicates (R1, R2, R3) of unsortable WEEE representative sample.

***PVC.*** The identification of PVC in the studied batch was achieved on the basis of TGA analysis. The first degradation observed in thermogravimetry (TG) and derivative thermogravimetry (DTG) curves at about 285 °C (Fig. 4b) could be attributed to the presence of PVC and allows the estimation of ~4.1 ± 1.4 wt % of PVC in the sample. Indeed, it has been demonstrated that the degradation of PVC occurs in two stages (McNeill et al., 1995): i) the first one (250–360 °C) corresponds to the dehydrochlorination and accounts for ~50 wt% of the weight loss, and ii) the second one (360–500 °C) is related to the polymer chains degradation. The latter accounts for ~25 wt% weight loss. PVC content in the representative sample determined from TGA is twice as high as estimated by the ATR-FTIR analysis on the 100 plastic fractions (Fig. 3b). On the other hand, ~1.9 ± 0.4 wt% of chlorine (Cl), coming mainly from PVC, was obtained from XRF analysis (Table 2). The over-estimated PVC concentration by TGA may be due to potential interactions between degradation products of the batch components that could enhance the dehydrochlorination rate of PVC, particularly in the presence of ABS and/or PET (Czégény et al., 2012).

*3.1.2.4. Additives, charges and fillers.* The complexity of the studied batch comes not only from the different types of polymers, as described above, but also from the numerous inorganic/organic additives commonly incorporated in plastic materials to improve their properties either mechanical, physico-chemical, thermal, rheological or even esthetic. TGA analysis (Fig. 4b) showed approximately 8.0 ± 0.3% under nitrogen residue, confirming the presence of an inorganic phase. XRF analysis of the studied batch has allowed a reliable screening of its elemental composition (Table 2). The validity of the sampling method is demonstrated by the low standard deviation of the replicates. Several additive systems were identified as a result of the elements examination.

Magnesium (Mg), aluminum (Al) and silicon (Si) are commonly used in the composition of mineral fillers, usually in the form of silicates such as talc (hydrated magnesium silicate, $Mg_3Si_4O_{10}(OH)_2$) or kaolin (hydrated aluminum silicate, $Al_2Si_2O_5(OH)_4$). Mg and Al elements can also be issued from the presence of hydrotalcite compounds ($Mg_6Al_2CO_3(OH)_{16}$, $4(H_2O)$), used as a heat co-stabilizer for PVC (Bao et al., 2008). Calcium carbonate ($CaCO_3$) is the main Ca-based molecule frequently used in plastic industry with the purpose to decrease the final cost of the material and increase its mechanical properties. Nonetheless, calcium oxide (CaO) in combination with silicon dioxide ($SiO_2$) and aluminum oxide ($Al_2O_3$), originated from fiberglass (Maris et al., 2015), should not be ignored.

The recorded concentration of total bromine (Br; 0.070 ± 0.002 wt%) along with that of the other regulated elements such as lead (Pb; 0.006 wt%) and chromium (Cr; 0.014 ± 0.002 wt%), complies with RoHS (Restriction of Hazardous Substances) regulation, hence allowing the recovery of the studied batch by means of mechanical recycling. Once again, the very small standard deviation reflects the reliability of the sampling method. It is worth mentioning that BFR-containing plastics were separated from the studied batch using an on-line X-ray detection as defined in the directive 2019/1021/EU (2019/1021/EU, 2019).

Br, antimony (Sb) and phosphorus (P) indicate the presence of flame retardants (FR) in the studied batch. Sb, in the form of antimony trioxide ($Sb_2O_3$), is used as a synergic agent of BFR thereby enhancing the bromine release from BFR by forming $Sb_2Br_3$ (Grause et al., 2010). Additionally, P-based FR such as phosphates, phosphites and melamine phosphates have been widely used in the last decades as value-added FR systems.

The small concentration of Zn (zinc) and Cr elements in the batch can be attributed to Ziegler-Natta and Philips catalysts used for polymerization process of PP and PE (Bichinho et al., 2005). Similarly, residual sodium persulfate ($Na_2S_2O_8$), a water-soluble initiator, used in the emulsion polymerization processes (Kumar and Gupta, 2003), can explain the presence of sodium (Na) and sulfur (S). Sulphites, are another S-based molecule commonly

**Table 2**
Weight % of the different elements detected in the unsortable WEEE representative sample as determined by XRF.

| Elements | Concentration (wt. %) | | Elements | Concentration (wt. %) | |
|---|---|---|---|---|---|
| | Average | Error* | | Average | Error* |
| H | 7.917 | 0.050 | Ba | 0.143 | 0.042 |
| C | 82.366 | 0.665 | S | 0.112 | 0.015 |
| N | 1.865 | 0.021 | Fe | 0.145 | 0.012 |
| O | 2.175 | 0.192 | Ni | 0.011 | 0.001 |
| Ca | 0.859 | 0.082 | Cu | 0.011 | 0.001 |
| Mg | 0.342 | 0.056 | Cr | 0.014 | 0.002 |
| Si | 0.646 | 0.046 | Zn | 0.072 | 0.004 |
| Al | 0.152 | 0.135 | Mn | 0.002 | 0.000 |
| Cl | 1.867 | 0.400 | Sn | 0.002 | 0.000 |
| Br | 0.070 | 0.002 | Pb | 0.006 | 0.000 |
| Sb | 0.114 | 0.021 | Na | 0.107 | 0.021 |
| Ti | 0.571 | 0.065 | K | 0.035 | 0.003 |
| P | 0.390 | 0.041 | Sr | 0.009 | 0.002 |

*The calculated error is based on three replicates

found in plastic parts because of their hydroperoxide inhibition properties.

The low Ti content (~0.57 ± 0.07 wt%), originated from titanium dioxide ($TiO_2$), is related to the fact that unsortable WEEE streams are mainly constituted of dark colored plastic fractions, whereas $TiO_2$ is usually used as white pigment in PC/ABS blends (Taurino et al., 2010).

Iron (Fe), nickel (Ni), and copper (Cu) XRF signals, can be explained by the presence of residual metallic parts that have not been removed during the sorting steps. Furthermore, the Fe-based barium ferrite ($BaFe_{12}O_{19}$) is frequently found in electrical equipment operating at microwave/GHz frequencies due to its electrical properties (Pullar, 2012).

The screening of the 500 Kg batch gives an interesting insight into the composition of a real unsortable post-consumer WEEE streams. The characterization of either bulk samples (~20 mm size) or batch representative samples has allowed a reliable quantification of the main polymers used in the manufacture of small EEE devices; styrene-based polymers (e.g. ABS, PS and HIPS), PP and PC account for more than 70% of the total organic components. The heterogeneity and complexity of the stream arise also from the detected inorganic/organic additives frequently used in the plastics industry. This phase accounts for 8 wt % and includes calcium carbonate, mineral fillers, and fiberglass. More importantly, the recorded concentration of the RoHS restricted substances enables the batch mechanical recycling.

### 3.2. Relevance of EB irradiation to mechanical properties of unsortable WEEE plastics

Given the complex composition of the studied batch, electron beam (EB) irradiation was considered as a means of compatibilization between the batch components. Indeed, processing a complex polymer blend may give rise to materials with poor mechanical properties as a consequence of polymers incompatibility and heterogeneity (Maris et al., 2018). Irradiation of a complex polymer blend results in *in-situ* cross-linking reactions at the interface leading to polymer compatibilization (Sonnier et al., 2012). From a potential industrial application perspective, EB-based ionizing radiation was adopted. Indeed, EB technology is already used on an industrial scale for commercial purposes, does not generate nuclear waste, is characterized by its short processing time and complies with restrictions on volatile organic compounds emission (International Irradiation Association, 2011).

In the present work, two experimental pathways were investigated; the first one has involved EB irradiation of micro-ground sample (<500 μm particle size) prior to tween-screw extrusion step, hereafter denoted as irradiated powder, while the second one has dealt with irradiated extruded pellets, hereafter denoted as irradiated pellets. Non-irradiated pellets, extruded irradiated powder and irradiated pellets were then injection molded and mechanically characterized. Fig. 5 illustrates tensile strength and impact toughness results on irradiated unsortable WEEE samples as a function of irradiation dose and experimental procedure. The applied irradiation on powder has not a significant effect on the mentioned properties. Except for elastic moduli (Fig. 5a), the mechanical behavior of the investigated samples highlights irradiation dose and process dependency; stress at yield (Fig. 5b) of irradiated pellets decreases after irradiation, while the EB irradiation undertaken on powder does not show a significant evolution of the mentioned property. Additionally, the irradiation dose is with no noteworthy impact on the irradiated powder elongation at break (Fig. 5c) compared to that on the irradiated pellets, where a drop of the elongation at break was observed. Regarding the impact toughness (Fig. 5d), the EB irradiation led to a slight decrease of the sample toughness median value regardless of the applied irradiation dose and the experimental procedure. Nevertheless, the wide range of the boxplot limits (i.e. Min-Max) of non-irradiated material highlights the material heterogeneity that probably hides the real effect of EB irradiation.

Based on these findings, it can be assumed that EB irradiation process does not really increase the adhesion through *in-situ* crosslinking and compatibilization between the different component phases of the investigated batch. Moreover, the decrease of elongation at break and impact toughness of the irradiated samples may result from a potential polymer chain degradation. In order to give more insight into this hypothesis, DSC analysis was carried out on injection molded bar specimens used for mechanical testing. The recorded DSC thermograms are displayed in Fig. 6. First, the heating DSC thermograms (Fig. 6a) of non-irradiated bars exhibit phase transitions similar to those for representative samples (Fig. 4a); two distinctive endothermic melting peaks around ~127 °C ($T_m$ PE) and ~164 °C ($T_m$ PP), as well as a styrene-based polymers glass transition at ~99 °C. On the contrary, the crystallization of PE component occurs at a delayed temperature (~131 °C), closer to that of PP, for non-irradiated processed sample (Fig. 6b), than for non-processed representative sample (Fig. S2). These observations might be indicative of PE dissolution in PP matrix in the molten state (Blom et al., 1998). Besides, EB irradiation, particularly at 200 kGy, leads PP melting point to shift meaningfully to a lower temperature ($T_m$ PP = ~154 °C) and PE melt enthalpy to decrease significantly (0.48 J/g for 200 kGy irradiated sample *vs.* 0.83 J/g for non-irradiated sample). In addition, the EB irradiation process gives rise to a single slightly shifted exothermic peak (Fig. 6b), representative of simultaneous crystallization of PP and PE, whereas it shows no impact on $T_g$ of the styrenic polymers. It should be noted that DSC analysis on bar samples injection molded from irradiated pellets (Fig. S3) exhibits a similar trend to that presented in Fig. 6 with a PE crystallization occurring later than that of PP resulting in a broader PP melt peak.

It has been demonstrated for PE/PP blends that the depression of both melting temperature and crystallinity rate indicates the miscibility phenomena (Li et al., 2001), and that potential chemical interactions between macroradicals of irradiated PP and PE are favorable during melt processing (Fel et al., 2016). However, it is worth pointing out that melt temperature decrease is also indicative of degraded polymers, and that crystallinity rate drop may be due to their crosslinking. Given the complex composition of the studied batch, DSC was not able to estimate the impact of irradiation on the other batch polymer components, that would have provided supporting explanations for the observed mechanical behavior of irradiated samples.

Other methods such as electron paramagnetic resonance (EPR) and l,l-diphenyl-2-picrylhydrazyl (DPPH) (unpublished results) failed to detect the persistence of macroradicals in irradiated samples. Several key assumptions can be made: (1) EPR spectra are difficult to interpret because of the complex batch composition; (2) The presence of Fe-based molecules gives rise to anisotropic EPR spectra as the sample position changes; (3) The remaining pigments in the batch hinder UV-absorbance of $DPPH^{\bullet}$ radicals; (4) Residual antioxidants and free radical scavengers react with $DPPH^{\bullet}$ radicals.

Based on all the observations and discussion in this section, it can be hypothesized that upon irradiation, PP undergoes $\beta$-chain scissions followed by crosslinking reactions with irradiated-PE during melt processing stages, which may explain the decrease in the elongation at break and impact toughness. On the other hand, although the irradiation may have led to free radical production, the subsequent *in-situ* crosslinking reactions were not efficient enough to allow compatibilization between the different polymer

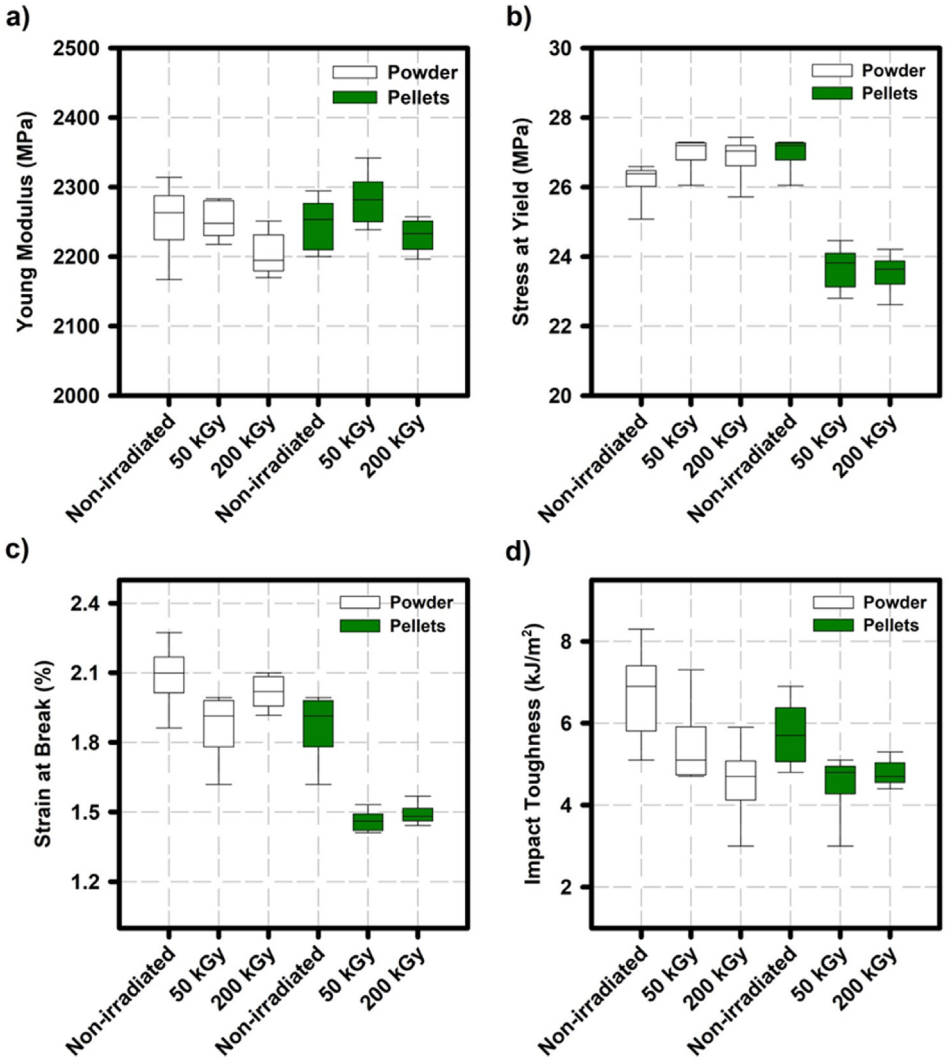


**Fig. 5.** a) Young modulus, b) stress at yield, c) strain at break and d) impact toughness for irradiated unsortable WEEE samples as a function of irradiation dose and experimental procedure (dog-bone specimens from irradiated powder or from irradiated pellets).

phases, and consequent mechanical performance improvement of the final material. This can be explained by the complex composition of the unsortable post-consumer WEEE stream and the presence of residual free radical scavengers.

## 4. Conclusions

Mechanical recycling of plastics derived from post-consumer WEEE is an important waste management strategy. However, ~40% of this waste stream, named unsortable, are rejected from the classical NIR sorting lines as they don't comply with the sorted plastic streams and also because of their dark color. For the first time, a comprehensive examination of a real unsortable WEEE fraction has been investigated in the present work. The screening of the studied batch composition, based on FTIR analysis of 100 plastic parts (~20 mm size) and physico-chemical characterization of representative samples, allowed a reliable quantification and identification of different polymer types; including mainly ~50% styrenic polymers, ~15% PP, and ~15% PC, and showed the existence of ~8 wt % inorganic phase (calcium carbonate, talc and fiberglass). Most importantly, the concentration of total bromine, lead and chromium, in agreement with RoHS (Restriction of Hazardous Substances) regulation, gives evidence for the batch mechanical recycling.

Given the heterogenous composition of the 500 kg batch under investigation, EB irradiation, as a means of compatibilization between the batch components, was investigated. The potential recycling of the studied batch was evaluated through mechanical properties as function of irradiation dose (50 and 200 kGy) and experimental procedure (irradiated powder and irradiated pellets). Unlike irradiated powder, a significant drop of the elongation at break and stress at yield was detected for irradiated pellets regardless of the applied dose. Nevertheless, the impact toughness property was found to decrease independently of the applied irradiation dose and the experimental procedure. DSC analysis have shown potential PP $\beta$-chain scissions followed by crosslinking reactions with irradiated-PE during melt processing stages. This study has provided evidence that the behavior difference between a EB-irradiated unsortable post-consumer WEEE stream and a EB-irradiated virgin polymers blend, reported in the literature, is due to the complex composition of the stream and the presence of residual free radical scavengers which hinder *in-situ* crosslinking reactions leading to the compatibilization between the different polymer phases. The present study shows that mechanical

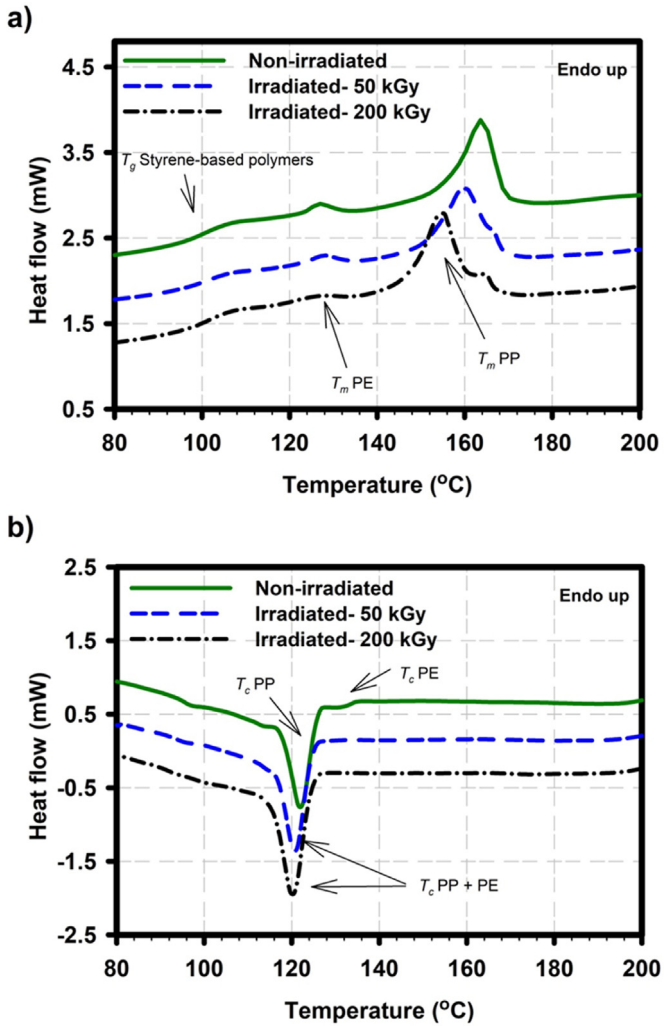


**Fig. 6.** DSC thermograms for bar specimens injection molded from irradiated then extruded powder at different irradiation dose (0, 50 and 200 kGy). a) 2nd heating cycle, and b) cooling cycle.

recycling simulation based on virgin polymer blend or sorted polymer waste is not representative of real post-consumer unsortable streams. This work may spur further studies on other ways of compatibilization in order to improve mechanical properties and cost-effectiveness.

## CRediT authorship contribution statement

**Imane Belyamani:** Conceptualization, Methodology, Validation, Formal analysis, Investigation, Data curation, Supervision, Writing - original draft, Writing - review & editing, Visualization. **Joachim Maris:** Conceptualization, Methodology, Validation, Formal analysis, Investigation, Data curation. **Sylvie Bourdon:** Conceptualization, Supervision, Writing - review & editing, Resources, Funding acquisition. **Jean-Michel Brossard:** Conceptualization, Validation, Supervision, Writing - review & editing, Resources, Funding acquisition. **Laurent Cauret:** Conceptualization, Methodology, Validation, Supervision. **Laurent Fontaine:** Conceptualization, Methodology, Validation, Supervision. **Véronique Montembault:** Conceptualization, Methodology, Validation, Project administration, Supervision, Writing - review & editing.

## Declaration of competing interest

The authors declare that they have no known competing financial interests or personal relationships that could have appeared to influence the work reported in this paper.

## Acknowledgments

We acknowledge financial support from Veolia Research & Innovation and ANRT (Association National de la Recherche et de la Technologie).

Additional Supporting Information may be found in the online version of this article.

## Appendix A. Supplementary data

Supplementary data to this article can be found online at https://doi.org/10.1016/j.jclepro.2021.126300.

## References

Afnor, 2018. XP CEN/TS 17188 standard: Prélèvement et échantillonnage de granulats.
Alwaeli, M., 2011. Economic calculus of the effectiveness of waste utilization processed as substitutes of primary materials. Environ. Protect. Eng. 37, 51–58.
Bao, Y., Zhi-ming, H., Shen-xing, L., Zhi-xue, W., 2008. Thermal stability, smoke emission and mechanical properties of poly (vinyl chloride)/hydrotalcite nanocomposites. Polym. Degrad. Stabil. 93, 448–455. https://doi.org/10.1016/j.polymdegradstab.2007.11.014.
Bichinho, K.M., Pires, G.P., Stedile, F.C., dos Santos, J.H.Z., Wolf, C.R., 2005. Determination of catalyst metal residues in polymers by X-ray fluorescence. Spectrochim. Acta Part B At. Spectrosc. 60, 599–604. https://doi.org/10.1016/j.sab.2004.11.012.
Blom, H.P., Teh, J.W., Bremner, T., Rudin, A., 1998. Isothermal and non-isothermal crystallization of PP: effect of annealing and of the addition of HDPE. Polymer 39, 4011–4022. https://doi.org/10.1016/S0032-3861(97)10305-6.
Bovea, M.D., Pérez-Belis, V., Ibáñez-Forés, V., Quemades-Beltrán, P., 2016. Disassembly properties and material characterisation of household small waste electric and electronic equipment. Waste Manag. 53, 225–236. https://doi.org/10.1016/j.wasman.2016.04.011.
Burillo, G., Clough, R.L., Czvikovszky, T., Guven, O., Le Moel, A., Liu, W., Singh, A., Yang, J., Zaharescu, T., 2002. Polymer recycling: potential application of radiation technology. Radiat. Phys. Chem. 64, 41–51. https://doi.org/10.1016/S0969-806X(01)00443-1.
Chancerel, P., Rotter, S., 2009. Recycling-oriented characterization of small waste electrical and electronic equipment. Waste Manag. 29, 2336–2352. https://doi.org/10.1016/j.wasman.2009.04.003.
Chmielewski, A.G., Haji-Saeid, M., Ahmed, S., 2005. Progress in radiation processing of polymers. Nucl. Instrum. Methods Phys. Res. Sect. B Beam Interact. Mater. At., Ionizing Radiation & Polymers 236, 44–54. https://doi.org/10.1016/j.nimb.2005.03.247.
Convention, Stockholm, 2017. Guidance on Best Available Techniques and Best Environmental Practices for the Recycling and Disposal of Wastes Containing Polybrominated Diphenyl Ethers (PBDEs) Listed under the Stockholm Convention on Persistent Organic Pollutants. Stockholm Convention.
Czégény, Z., Jakab, E., Blazsó, M., Bhaskar, T., Sakata, Y., 2012. Thermal decomposition of polymer mixtures of PVC, PET and ABS containing brominated flame retardant: formation of chlorinated and brominated organic compounds. J. Anal. Appl. Pyrolysis 96, 69–77. https://doi.org/10.1016/j.jaap.2012.03.006.
Dimitrakakis, E., Janz, A., Bilitewski, B., Gidarakos, E., 2009. Small WEEE: determining recyclables and hazardous substances in plastics. J. Hazard Mater. 161, 913–919. https://doi.org/10.1016/j.jhazmat.2008.04.054.
Dolores, A.J., Lasco, J.D.D., Bertiz, T.M., Lamar, K.M., 2020. In: Compressive Strength and Bulk Density of Concrete Hollow Blocks (CHB) Infused with Low-Density Polyethylene (LDPE) Pellets, vol. 6, pp. 1932–1943. https://doi.org/10.28991/cej-2020-03091593.
Drobny, J.G., 2010. Radiation Technology for Polymers. CRC press.
Epsztein, S.R., de Fombelle, M.A.J., Falher, T., Jouannet, D., Gallone, T., Cauret, L., 2014. Substitution of Virgin Material by Recycled Material from End-Of-Life Vehicle (ELV). Presented at the Key Engineering Materials. Trans Tech Publ, pp. 836–843. https://doi.org/10.4028/www.scientific.net/KEM.611-612.836.
2012/19/EU, 2012. Directive 2012/19/EU of the European Parliament and of the Council of 4 July 2012 on Waste Electrical and Electronic Equipment.
2019/1021/EU, 2019. Regulation (EU) 2019/1021 of the European Parliament and of the Council - of 20 June 2019 - on Persistent Organic Pollutants.
Fel, E., Khrouz, L., Massardier, V., Cassagnau, P., Bonneviot, L., 2016. Comparative study of gamma-irradiated PP and PE polyolefins part 2: properties of PP/PE blends obtained by reactive processing with radicals obtained by high shear or

gamma-irradiation. Polymer 82, 217–227. https://doi.org/10.1016/j.polymer.2015.10.070.
Gardette, J.-L., Mailhot, B., Lemaire, J., 1995. Photooxidation mechanisms of styrenic polymers. Polym. Degrad. Stabil. 48, 457–470. https://doi.org/10.1016/0141-3910(95)00113-Z.
Ghorbel, E., Hadriche, I., Casalino, G., Masmoudi, N., 2014. Characterization of thermo-mechanical and fracture behaviors of thermoplastic polymers. Materials 7, 375–398. https://doi.org/10.3390/ma7010375.
Gramatyka, P., Nowosielski, R., Sakiewicz, P., 2007. Recycling of waste electrical and electronic equipment. J. Achiev. Mater. Manuf. Eng. 20, 535–538. https://doi.org/10.12691/ajmr-6-1-3.
Grause, G., Ishibashi, J., Kameda, T., Bhaskar, T., Yoshioka, T., 2010. Kinetic studies of the decomposition of flame retardant containing high-impact polystyrene. Polym. Degrad. Stabil. 95, 1129–1137. https://doi.org/10.1016/j.polymdegradstab.2010.02.008.
Gu, J., Xu, H., Wu, C., 2014. Thermal and crystallization properties of HDPE and HDPE/PP blends modified with DCP. Adv. Polym. Technol. 33 https://doi.org/10.1002/adv.21384.
Gy, P., 1998. Sampling for Analytical Purposes. John Wiley & Sons.
Hamaide, T., Deterre, R., Feller, J.-F., 2014. Environmental Impact of Polymers. John Wiley & Sons.
Hennebert, P., 2017. WEEE Plastic Sorting for Bromine Content Is Essential to Enforce EU Regulation.
Huy, T.A., Adhikari, R., Lüpke, T., Henning, S., Michler, G.H., 2004. Molecular deformation mechanisms of isotactic polypropylene in α-and β-crystal forms by FTIR spectroscopy. J. Polym. Sci., Part B: Polym. Phys. 42, 4478–4488. https://doi.org/10.1002/polb.20117.
International Irradiation Association, 2011. Industrial Radiation with Electron Beams and X-Rays.
Ismail, H., Hanafiah, M.M., 2019. An overview of LCA application in WEEE management: current practices, progress and challenges. J. Clean. Prod. 232, 79–93. https://doi.org/10.1016/j.jclepro.2019.05.329.
Kang, H.-Y., Schoenung, J.M., 2005. Electronic waste recycling: a review of U.S. infrastructure and technology options. Resour. Conserv. Recycl. 45, 368–400. https://doi.org/10.1016/j.resconrec.2005.06.001.
Karahaliou, E., Tarantili, P., 2009. Stability of ABS compounds subjected to repeated cycles of extrusion processing. Polym. Eng. Sci. 49, 2269–2275. https://doi.org/10.1002/pen.21480.
Kumar, A., Gupta, R.K., 2003. Fundamentals of Polymer Engineering. Marcel Dekker, Inc, New York.
Kyere, V.N., Greve, K., Atiemo, S.M., Amoako, D., Kwame Aboh, I.J., Cheabu, B., 2018. Contamination and health risk assessment of exposure to heavy metals in soils from informal E-waste recycling site in Ghana. Emerg. Sci. J. 2, 428–436. https://doi.org/10.28991/esj-2018-01162.
Lacoste, J., Delor, F., Pilichowski, J., Singh, R., Prasad, A.V., Sivaram, S., 1996. Polybutadiene content and microstructure in high impact polystyrene. J. Appl. Polym. Sci. 59, 953–959. https://doi.org/10.1002/(SICI)1097-4628(19960207)59:6<953::AID-APP7>3.0.CO;2-O.
Lambla, M., Seadan, M., 1992. Interfacial grafting and crosslinking by free radical reactions in polymer blends. Polym. Eng. Sci. 32, 1687–1694. https://doi.org/10.1002/pen.760322206.
Lambla, M., Seadan, M., 1993. Reactive blending of polymers by interfacial free-radical grafting. Makromol. Chem. Macromol. Symp. 69, 99–123. https://doi.org/10.1002/masy.19930690112.
Li, J., Shanks, R.A., Olley, R.H., Greenway, G.R., 2001. Miscibility and isothermal crystallisation of polypropylene in polyethylene melts. Polymer 42, 7685–7694. https://doi.org/10.1016/S0032-3861(01)00248-8.
Li, R., Zhang, X., Zhou, L., Dong, J., Wang, D., 2009. In situ compatibilization of polypropylene/polystyrene blend by controlled degradation and reactive extrusion. J. Appl. Polym. Sci. 111, 826–832. https://doi.org/10.1002/app.29118.
Li, Y., Wu, X., Song, J., Li, J., Shao, Q., Cao, N., Lu, N., Guo, Z., 2017. Reparation of recycled acrylonitrile-butadiene-styrene by pyromellitic dianhydride: reparation performance evaluation and property analysis. Polymer 124, 41–47. https://doi.org/10.1016/j.polymer.2017.07.042.
Li, J., Li, C., Liao, Q., Xu, Z., 2019. Environmentally-friendly technology for rapid online recycling of acrylonitrile-butadiene-styrene, polystyrene and polypropylene using near-infrared spectroscopy. J. Clean. Prod. 213, 838–844. https://doi.org/10.1016/j.jclepro.2018.12.160.
Liang, C.Y., Krimm, S., 1958. Infrared spectra of high polymers. VI. Polystyrene. J. Polym. Sci. 27, 241–254. https://doi.org/10.1002/pol.1958.1202711520.
Maris, E., Botané, P., Wavrer, P., Froelich, D., 2015. Characterizing plastics originating from WEEE: a case study in France. Miner. Eng., Sustainable Minerals 76, 28–37. https://doi.org/10.1016/j.mineng.2014.12.034.
Maris, J., Bourdon, S., Brossard, J.-M., Cauret, L., Fontaine, L., Montembault, V., 2018. Mechanical recycling: compatibilization of mixed thermoplastic wastes. Polym. Degrad. Stabil. 147, 245–266. https://doi.org/10.1016/j.polymdegradstab.2017.11.001.
Martinho, G., Pires, A., Saraiva, L., Ribeiro, R., 2012. Composition of plastics from waste electrical and electronic equipment (WEEE) by direct sampling. Waste Manag. 32, 1213–1217. https://doi.org/10.1016/j.wasman.2012.02.010.
McNeill, I.C., Memetea, L., Cole, W.J., 1995. A study of the products of PVC thermal degradation. Polym. Degrad. Stabil. 49, 181–191. https://doi.org/10.1016/0141-3910(95)00064-S.
Menad, N.-E., 2016. Chapter 3 - physical separation processes in waste electrical and electronic equipment recycling. In: Chagnes, A., Cote, G., Ekberg, C., Nilsson, M., Retegan, T. (Eds.), WEEE Recycling. Elsevier, pp. 53–74. https://doi.org/10.1016/B978-0-12-803363-0.00003-1.
Milad, A., Ali, A.S.B., Yusoff, N.I.M., 2020. A review of the utilisation of recycled waste material as an alternative modifier in asphalt mixtures. J. Civ. Eng. 6, 42–60. https://doi.org/10.28991/cej-2020-SP(EMCE)-05.
Munteanu, S., Vasile, C., 2005. Spectral and thermal characterization of styrene-butadiene copolymers with different architectures. J. Optoelectron. Adv. Mater. 7, 3135.
Numata, S., Fujii, Y., 1995. Improved flexural properties of polymer blends by mixing with a multifunctional monomer and crosslinking with gamma-rays. Plast., Rubber Compos. Process. Appl. 5, 293–300.
Parajuly, K., Wenzel, H., 2017. Potential for circular economy in household WEEE management. J. Clean. Prod. 151, 272–285. https://doi.org/10.1016/j.jclepro.2017.03.045.
Pullar, R.C., 2012. Hexagonal ferrites: a review of the synthesis, properties and applications of hexaferrite ceramics. Prog. Mater. Sci. 57, 1191–1334. https://doi.org/10.1016/j.pmatsci.2012.04.001.
Sahajwalla, V., Gaikwad, V., 2018. The present and future of e-waste plastics recycling. Curr. Opin. Green sustain. Chem., reuse and recycling/UN SGDs: how can sustainable chemistry contribute? Green Chemistry in Education 13, 102–107. https://doi.org/10.1016/j.cogsc.2018.06.006.
Said, H.M., Khafaga, M.R., El-Naggar, A.W.M., 2013. Compatibilization of poly (ethylene terephthalate)/low density polyethylene blends by gamma irradiation and graft copolymers. Arab J. Nucl. Sci. Appl. 46, 56–69.
Satapathy, S., Chattopadhyay, S., Chakrabarty, K.K., Nag, A., Tiwari, K.N., Tikku, V.K., Nando, G.B., 2006. Studies on the effect of electron beam irradiation on waste polyethylene and its blends with virgin polyethylene. J. Appl. Polym. Sci. 101, 715–726. https://doi.org/10.1002/app.23970.
Silas, R.S., Yates, J., Thornton, V., 1959. Determination of unsaturation distribution in polybutadienes by infrared spectrometry. Anal. Chem. 31, 529–532. https://doi.org/10.1021/ac50164a022.
Sonnier, R., Taguet, A., Rouif, S., 2012. Modification of polymer blends by E-beam and Gamma-irradiation. In: Functional Polymer Blends: Synthesis, Properties, and Performance. Boca Raton CRC Press, pp. 261–304.
Stenvall, E., Tostar, S., Boldizar, A., Foreman, M.R.S., Möller, K., 2013. An analysis of the composition and metal contamination of plastics from waste electrical and electronic equipment (WEEE). Waste Manag. 33, 915–922. https://doi.org/10.1016/j.wasman.2012.12.022.
Taurino, R., Pozzi, P., Zanasi, T., 2010. Facile characterization of polymer fractions from waste electrical and electronic equipment (WEEE) for mechanical recycling. Waste Manag. 30, 2601–2607. https://doi.org/10.1016/j.wasman.2010.07.014.
Tostar, S., Stenvall, E., Foreman, M., Boldizar, A., 2016. The influence of compatibilizer addition and gamma irradiation on mechanical and rheological properties of a recycled WEEE plastics blend. Recycling 1, 101–110. https://doi.org/10.3390/recycling1010101.
Utracki, L.A., 2002. Compatibilization of polymer blends. Can. J. Chem. Eng. 80, 1008–1016. https://doi.org/10.1002/cjce.5450800601.
Vazquez, Y.V., Barbosa, S.E., 2016. Recycling of mixed plastic waste from electrical and electronic equipment. Added value by compatibilization. Waste Manag. 53, 196–203. https://doi.org/10.1016/j.wasman.2016.04.022.
Vilaplana, F., Ribes-Greus, A., Karlsson, S., 2006. Degradation of recycled high-impact polystyrene. Simulation by reprocessing and thermo-oxidation. Polym. Degrad. Stabil. 91, 2163–2170. https://doi.org/10.1016/j.polymdegradstab.2006.01.007.
Vivier, T., Xanthos, M., 1994. Peroxide modification of a multicomponent polymer blend with potential applications in recycling. J. Appl. Polym. Sci. 54, 569–575. https://doi.org/10.1002/app.1994.070540507.
Wang, R., Xu, Z., 2014. Recycling of non-metallic fractions from waste electrical and electronic equipment (WEEE): a review. Waste Manag. 34, 1455–1469. https://doi.org/10.1016/j.wasman.2014.03.004.
Widmer, R., Oswald-Krapf, H., Sinha-Khetriwal, D., Schnellmann, M., Böni, H., 2005. Global perspectives on e-waste. Environ. Impact Assess. Rev., Environmental and Social Impacts of Electronic Waste Recycling 25, 436–458. https://doi.org/10.1016/j.eiar.2005.04.001.
Xanthos, M., Dagli, S.S., 1991. Compatibilization of polymer blends by reactive processing. Polym. Eng. Sci. 31, 929–935. https://doi.org/10.1002/pen.760311302.
Zhu, Z., Kelley, M.J., 2005. IR spectroscopic investigation of the effect of deep UV irradiation on PET films. Polymer 46, 8883–8891. https://doi.org/10.1016/j.polymer.2005.05.135.